Ref. Ares(2022)3766416 - 18/05/2022

Project ID: **Fly-Radar**

Project Title: **Low-frequency multi-mode (SAR and penetrating) radar onboard light-weight UAV for Earth and Planetary exploration**

Call: **H2020-MSCA-RISE-2020**

WP1 –
Mars Surface and subsurface analyses and terrestrial analogs

D1.3: Mars surface and subsurface and physical model for radar investigation

Lead contributor	UCBL (4 – Université Claude Bernard Lyon 1)
Other contributors	

Due date	30 April 2022
Delivery date	18 May 2022
Deliverable type	Report[1]
Dissemination level	PU

Document History

Version	Date	Description
V1.0	18 May 2022	First version reviewed by all

This project has received funding from the European Union's Horizon 2020 research and innovation programme under MSCA-RISE2020 grant agreement No 101007973.

Publishable Summary

The radargrams produced by the FlyRadar system will need to be inverted to produce the most reliable geometry and permittivity estimates possible. Inversion techniques are based on radar equations that describe how signal strength evolves along its path from the transmitter to the target and back to the receiver.
If external data are available, such as the measurement of layer thickness for example, it will be possible to estimate the permittivity of these layers from the return times of the signal to the sensor. Other techniques have been developed that jointly invert the geometry and the permittivity of the underground from a radargram. These techniques are based either on the characteristics of the diffraction hyperbolas, or on the intensities of the signals received by the radar. Other techniques such as deep learning have not yet been used to process geological data. However, they seem promising on the available examples.

1. Introduction

The main objective of FlyRadar is the development of a drone carrying a radar capable of imaging the underground. The data produced by the radar will be used to identify the geometry of the underground structures and also, if possible, to characterize the rocks that make up these geometries.
The radar records the echo of the waves it emits on discontinuities of dielectric permittivity. It therefore records the time taken by the wave to go from the emission source to the reception point, passing through the reflective discontinuity. This time will vary according to the reception distance and the speed of the electromagnetic waves in the basement. If the radar is in Nadir view (vertical observation):

$$t = \frac{2h}{v} \quad (1)$$

With *h*, depth of the permittivity discontinuity, *t* the travel time of the wave from the source to the discontinuity and back to the receiver, *v* speed of the electromagnetic waves. Knowing the speed *v*, it is easy to invert the time signal in terms of the geometry of structures. However, the speed of electromagnetic waves in the underground is variable depending on the nature of the rocks and their geo-mechanical properties (e.g. Brouet et al., 2019). The speed *v*, therefore, constitutes, with the depth *h*, an unknown factor of the problem that it is necessary to resolve in order to best invert the temporal signal recorded by the radar.
On Earth, the use of GPR is particularly developed to identify subsurface structures (e.g. Girardi et al., 2010) whether for scientific (geology, glaciology, archaeology, etc.) or applied (geotechnics, hydrogeology, etc.) purposes. In most cases, the nature and properties of the underground are well known. The speed of electromagnetic waves is therefore generally well controlled. If this is not the case, it is also possible to carry out wave velocity measurements in the laboratory on samples from the study area (e.g. ElShafie and Heggy, 2013). The problem can therefore be completely defined on Earth, allowing the precise representation of the geometries of the underground.
On Mars, the nature of surface rocks can be estimated from geomorphological data associated with hyperspectral imagery data and sometimes thermal imagery. These data allow to frame the speeds of the electromagnetic waves. However, the geometry of the subsoil is difficult to determine and the speed of the electromagnetic waves does not only depend on the nature of the rocks but also on their porosity, their possible water content and other impurities. Velocity estimates therefore remain marred by a margin of uncertainty. It is more difficult to accurately represent the geometries of the underground on Mars than on the Earth.
Joint geometry-velocity inversion methods have been developed (e.g. Berthelier et al., 2003; Petinelli et al., 2007; Alberti et al., 2012) on the model of seismic inversion methods. The first family of methods is based on the prior determination of a geometry from images or 3D data to estimate a permittivity value. Other families of methods use the echoes returned by an object observed from several distances. Finally, techniques based on Deep Learning have recently appeared and constitute a new approach to joint geometry-dielectric properties inversion.

This project has received funding from the European Union's Horizon 2020 research and innovation programme under MSCA-RISE2020 grant agreement No 101007973.

2. Reminders on radar physics

A radar (RAdio Detection And Ranging) is an active remote sensing system using electromagnetic waves capable of reflecting on discontinuities. The transmission system is associated with a system for receiving reflected waves. To the first order, knowing the speed of the electromagnetic waves in the medium they cross, it is possible to estimate the distance of the reflective object (Eq. 1).
The radar equation (e.g. Lynn, 1986) describes the path of energy from the source to the target and back. The energy of the source depends on the power of the radar and the gain of the antenna. The surface energy of the wave front decreases progressively with the square of the distance. Part of this wave front encounters the target with a certain effective area. A wave train returns to the device. The energy of this secondary source also decreases with the square of the distance. If the ground is rough some of the energy will radiate and be lost to the receiver.

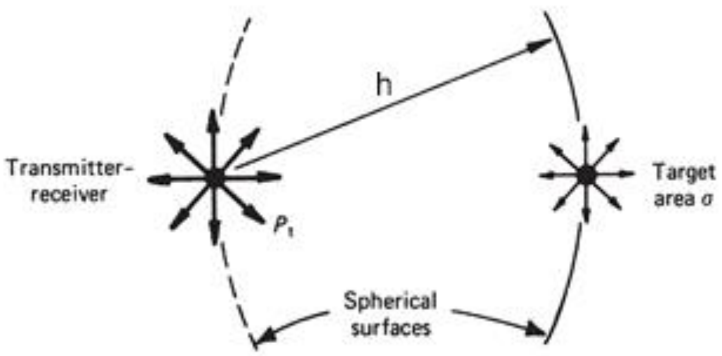

Figure 1: Diagram of a radar system and its target used to calculate the "radar equation" (modified after Lynn, 1986).

The radar equation describes the power loss between source and receiver. Without going into the details of the calculation (e.g. Lynn, 1987) the power P_r received by the radar depends on the characteristics of the source, the distance to the target, the properties of the medium in which the waves propagate and the properties of the target.

$$P_r = f(source - receiver, distance, propagation\ medium, target) \quad (2)$$

The source is characterized by the emitted wavelength and by the power of the transmitter modulated by the gain of the antenna. The receiver is characterized by its sensitivity which partly depends on the gain of the receiving antenna. For a monostatic device, the transmitting antenna is also the receiving antenna. Gain in emission is the same as the gain in reception.
If the emission and backscatter sources are considered as point sources, the power flux-density will decrease with the square of the distance to the target. By combining the decay of the emission towards the target with the decay of the backscatter towards the receiver, the power decreases with the fourth power of the distance between the source and the target.
The electromagnetic wave will propagate in a medium characterized by its dielectric properties. The permittivity defines the speed of the wave in the medium as well as the attenuation of the signal along the path of the wave. The effects of permittivity and the factors that control it are discussed in Part 3.
The target is, to first order, a discontinuity of the permittivity. Part of the waves will refract and continue its course while another will be backscattered. The backscattered power will depend on the permittivity contrast between the target and the propagation medium as well as the surface properties of the target and in particular its roughness. Indeed, the waves are reflected in a specular way on an ideally flat surface (not rough) whereas they will be backscattered on a rough surface (fig. 2). The roughness of the interface between the two media will therefore be an important parameter for controlling the backscattered intensity.

This project has received funding from the European Union's Horizon 2020 research and innovation programme under MSCA-RISE2020 grant agreement No 101007973.

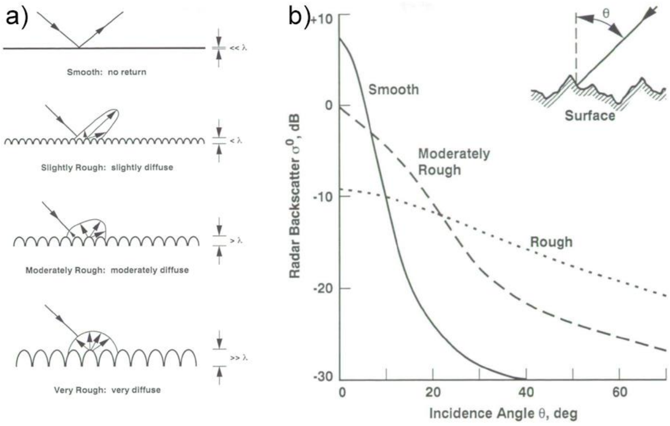

Figure 2: a) Effect of target roughness on radar signal backscatter. The rougher the surface, the more the signal is backscattered. b) Backscattered intensity as a function of viewing angle. Backscatter increases the intensity of the backscattered signal at wide viewing angles on rough surfaces (from Ford et al., 1993).

3. Permittivity

The developments of Maxwell's equations in connection with the radar method will not be given later. The interested reader will refer for example to Koslov et al. (1986) or Grima (2011). The following sections describe the rock parameters that control the radar signal. An electromagnetic wave will be transmitted in a rocky material with a given speed, *v*. This wave will also see its amplitude decrease. This decrease in intensity is added to the decreases in the radar signal described in part 2. These two effects depend on the value of the dielectric permittivity of the medium crossed. This permittivity is commonly defined as a complex number [ε ', tanδ] for which the real part describes the relations between the speed of waves and the speed of light:

$$v = \frac{c}{\sqrt{\varepsilon\prime}} \quad (3)$$

With *v*, speed of the electromagnetic wave, c, speed of light in vacuum, ε', permittivity of the material.
The imaginary part of the permittivity is called the loss tangent. It describes the attenuation of the wave in the medium crossed, which is very low in dielectric materials such as rocks. Grima et al. (2009) measures the loss tangent of the Martian north polar cap to deduce the impurity content.
Thereafter, we will name "permittivity" the real part of the total permittivity, and we will symbolize it by ε. The ranges of permittivities are given for common materials in table 1. The rocks present a contrast in permittivity which does not allow them to be discriminated. On Earth, knowledge of the geological environment generally makes it possible to overcome the question of determining the rocks. On Mars, the question is more delicate to resolve. It is necessary to rely on geomorphological observations or hyperspectral measurements to define the geological context.

This project has received funding from the European Union's Horizon 2020 research and innovation programme under MSCA-RISE2020 grant agreement No 101007973.

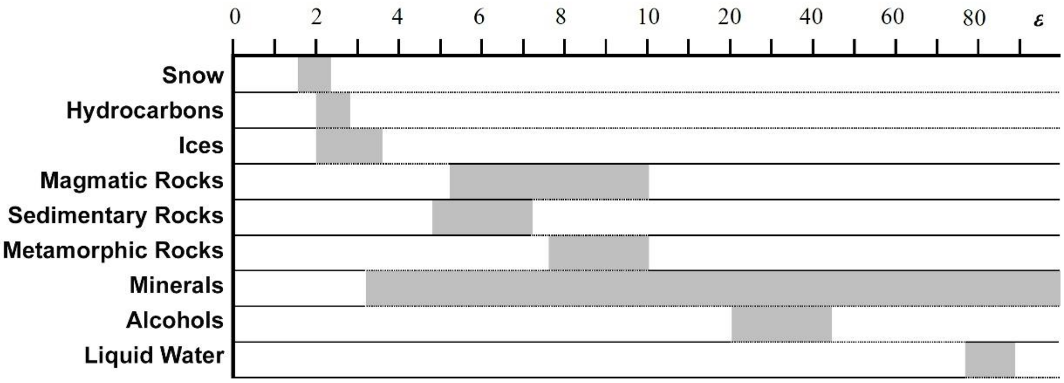

Table 1: Permittivity range for common materials (modified from Grima, 2011).

In a rocky material, the permittivity depends to the first order on the nature of this material. The value of the permittivity will however be modulated by external factors, such as the content, the observation wavelength, the temperature and the impurity content. The variation of permittivity with frequency can be approximated with Debye's equation. Applied to rocks and for wavelength values used in sounding radars, Debye's equation shows a weak dependence of permittivity on wavelength.

The relationships between temperature and permittivity are established experimentally (e.g. Heggy et al., 2003). There are a few results that show that low Martian temperatures do not significantly change permittivity values.

Impurities, such as voids, will play a more important role than temperature and observation wavelength. Loyenga's model (1965) is based on the impurity volume fraction to estimate the permittivity of the mixture:

$$\varepsilon_e^{1/3} = (1 - f)\varepsilon_m^{1/3} + f\varepsilon_i^{1/3} \quad (4)$$

With f, volume fraction of component i, ε_i, permittivity of component i, ε_m permittivity of the matrix and ε_e permittivity of the mixture.

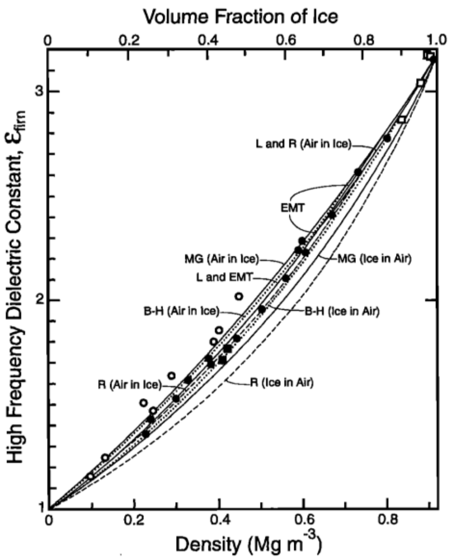

Figure 3: Variation of permittivity as a function of the ice fraction in a firn. The curves represent different mixing models including the Looyenga model (1965) and the points represent in situ measurements. Note the good agreement between observations and models (according to Wilhelms, 2005).

This project has received funding from the European Union's Horizon 2020 research and innovation programme under MSCA-RISE2020 grant agreement No 101007973.

4. Inversion of radargrams for the study of planetary undergrounds

The product from a radar is a radargram. It is a graphic representation which gives in abscissa a length corresponding to the path of the device and in ordinate a time corresponding to the reflections of the signal recorded by the device. The abscissa is therefore a length while the ordinate is a time. The objective is to transform the ordinate axis in depth to obtain a geometric representation of the underground. This is the migration operation.
According to equation (1), this operation is easy if we know *a priori* the permittivity of the underground. It will suffice to transform the time scale into distance. However, this case is rare. As we have seen in the previous paragraphs, the permittivity will vary not only according to the nature of the ground but also according to the content of impurities.
There are several techniques to estimate the permittivity from a radargram. The simplest consists in setting the radargram on geometric elements visible on the surface (4.1). A second technique consists in modeling the 3D geometry of the underground (4.2). It is also possible to calculate the subsoil velocity from hyperbolic signatures (4.3) or from the ration between the emitted power to the received power (4.4). In recent years, techniques based on deep learning have appeared (4.5).

4.1 Radargram inversion using external geometric data

4.1.1 Example on an Eolian Dune

From layer thickness measurements produced from topographic and imagery data, it is possible to propose the following method. From a digital terrain model (DTM – matrix of values describing the topography of a place) and an orthorectified image (image for which the distortions due to the topography have been removed) it is possible to estimate the thickness of this layer. The process can be described on the example of a dune (Fig. 4).

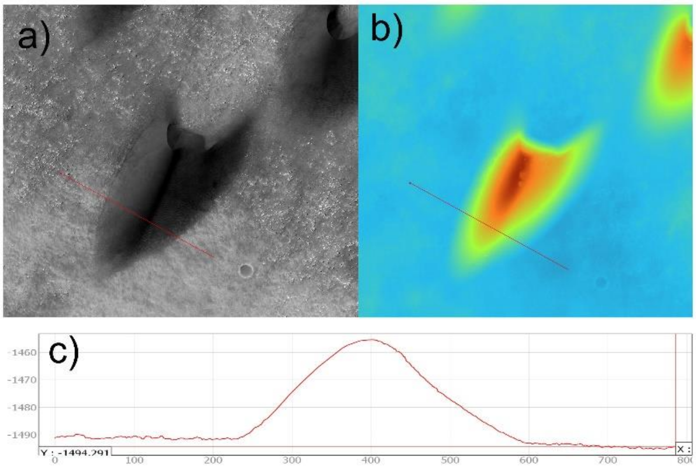

Figure 4: a) Barkhane in the Arkhangelsky Crater Dunes on Mars (41.09°S, 335.21°E). b) Digital Elevation Model of the Barkhane field (Hirise Team - https://www.uahirise.org/dtm/). C) Section of the barkhane. The length of the section gives the scale of the images.

We do not have a radargram for the dune represented in figure 4. For the example, figure 5 gives the image of a radargram of a terrestrial dune. The reflectors are perfectly identifiable. The base of the dune is represented by a strong horizontal reflector. By combining the topography of the dune with the temporal data of the radargram, it is possible to estimate the speed of the waves in the dune and to deduce the permittivity of the material composing the dune. In this example, the estimated permittivity will be an average permittivity taking into account the porosity of the sand as well as the oblique discontinuities visible on the radargram.

This project has received funding from the European Union's Horizon 2020 research and innovation programme under MSCA-RISE2020 grant agreement No 101007973.

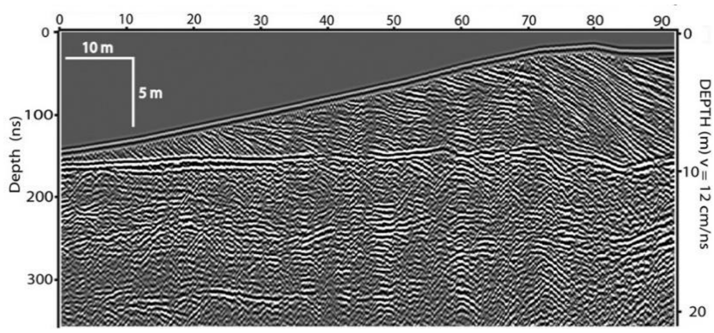

Figure 5: Radargram of a dune at Napeague, NY, USA from GPR (Girardi et al., 2010). Notice that the vertical axes are labelled in time on left and in distance on right. Notice also the strong sub-horizontal reflector visible at the base of the dune.

This estimate will be marred by an uncertainty which depends on the uncertainty on the propagation time, on the uncertainty on the measurement of the thickness of the sand, on the uncertainty of the permittivity on the non-porous rock.
The uncertainty on the propagation time measurement is a function of the sampling frequency (Bramson et al., 2015). The uncertainty on the thickness of sand will depend on the accuracy of the DEM. This accuracy is generally estimated at 0.25m for Hirise DEM's. The other geometrical parameter, which is more difficult to estimate, is the position of the substratum. We can estimate that it is horizontal, that it is oblique or even irregular without having any precise constraint on the model. The simplest is a plane oblique estimate. The nature of the material is the last uncertainty of the problem. Martian data shows that the dunes are made up of basalt sand. On such an example it is therefore possible to estimate, in addition to the internal geometry of the dune, the porosity of the sand that constitutes it.

4.1.2 Example on sedimentary layers

The surface of Mars is locally covered by sedimentary deposits that are clearly identifiable on satellite images (fig. 6). From a radargram and the thickness of the sedimentary layers. It will be possible to estimate the permittivity of the sedimentary material.

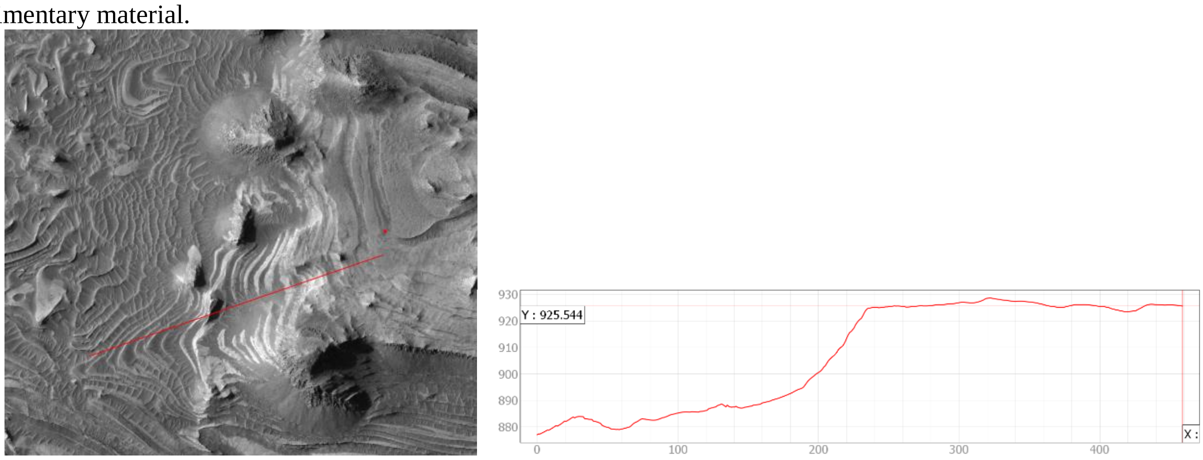

Figure 6: Martian sedimentary deposit (Est Chandor Chasma – Hirise image https://www.uahirise.org/dtm/) and cross section according to DEM produced by Hirise Team. Note the clearly visible layers in the image. The length of the section (500 m) gives the scale.

This project has received funding from the European Union's Horizon 2020 research and innovation programme under MSCA-RISE2020 grant agreement No 101007973.

4.2 Radargram inversion by modeling the geometry of the studied object

The following example is taken from the work of Grima et al., (2009) who use Sharad data on board the Mars Reconnaissance Orbiter to estimate the impurity content of the ice of the northern polar cap of Mars (fig. 7). The authors model the 3D geometry of the interface between the bedrock and the cap from the altitudes of the ice-rock interface measured around the perimeter of the cap. From the characteristics of the radar signals recorded on the available Sharad profiles and the modeled thicknesses of the ice cap, the authors estimate the permittivity of the ice as well as its loss tangent. As the values measured are close to those of pure ice, they estimate that the impurity content is low in the North ice cap.

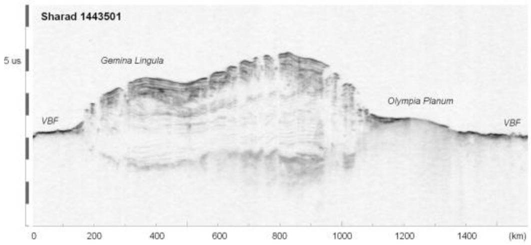

Figure 7: example of Sharad profile through the North polar cap. The vertical axis is time. Note the reflectors between the cap and the bedrock (Grima, 2009).

4.3 Coupled geometry-permittivity inversion methods

4.3.1 Methods based on diffraction hyperbolas

A class of coupled geometry-permittivity inversion methods uses diffracting element geometric properties to first estimate wave velocities to deduce permittivities and then use the velocity estimates to migrate the radargrams to obtain sections of the underground. The techniques are very similar to those used for the migration of seismic refraction profiles. The basic elements of the method are given in figure 8.

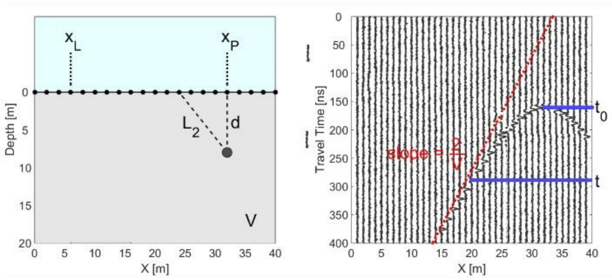

Figure 8: a diffracting object is located in a homogeneous subsoil. The radar echo of this object appears long before the radar is over the object. The typical signature is a diffraction hyperbola whose slope is inversely proportional to the wave velocity in the homogeneous medium.(modified from https://em.geosci.xyz/content/geophysical_surveys/gpr/physics.html - last view the 12/05/2022).

A diffracting object located in a homogeneous underground will have a characteristic signature. "Diffraction hyperbolas" will appear on the radargram. These hyperbolas are produced by the radar echoes on the object appearing before and after the radar is directly above it. Geometric considerations show that the slope of the hyperbola which appears on the radargram is inversely proportional to the speed of the waves.

These considerations form the basis of inversion techniques. Liu et al. (2023) propose an inversion method based on this concept. The difficulties to be solved consist in developing an effective filter capable of distinguishing the refraction hyperbolas of the reflected waves as well as knowing the shape of the radar pulse.

This project has received funding from the European Union's Horizon 2020 research and innovation programme under MSCA-RISE2020 grant agreement No 101007973.

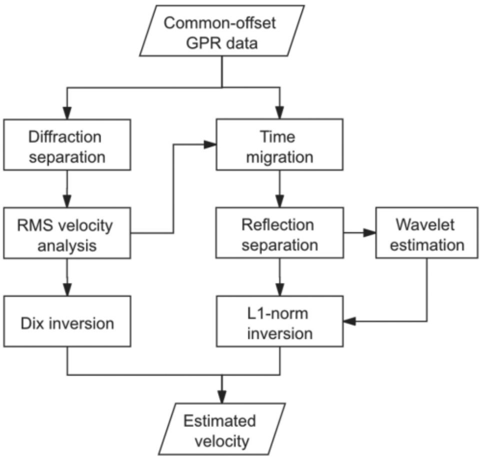

Figure 9: Flowchart illustrating the method proposed by Liu et al. (2022) for inversion of GPR data.

4.3.2 Methods based on the intensity of the signal reflected on the interfaces

A radar wave arriving at the surface of a planet will be partly reflected, partly diffracted by the surface roughness and partly transmitted into the planet (figure 10). The transmitted wave, when it encounters a permittivity interface, will be partly reflected back to the surface, partly diffracted by roughness and partly transmitted deeper into the planet's crust. The intensity of the first signal that returns to the radar depends on the permittivity contrast between the atmosphere and the first rock layer as well as the surface roughness. The intensity of the signal marking the reflection on the second interface will also depend on the permittivity contrast between the two rock layers as well as the roughness of this interface. The intensity of the signal received by the sensor is therefore a function of the geometry of the system (cf eq. 2) as well as of the permittivity contrast between the layers. If it is possible to measure or model the roughness of the interfaces, then it is possible to estimate the permittivity of the two outermost layers of the planet.

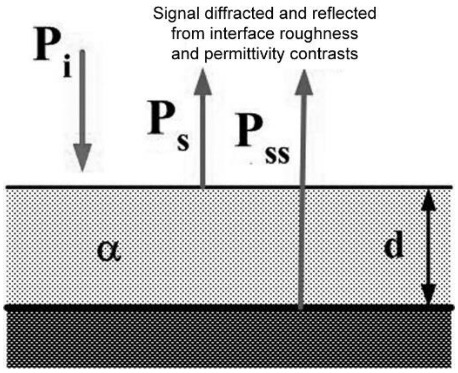

Figure 10: Electromagnetic model of the surface of a planet (modified after Alberti et al., 2012).

This method is efficient for determining the geometry and dielectric properties of horizontal layers whose roughness can be measured or estimated (Picardi et al., 2008).

4.3.3 Methods based on Deep Learning

Liu et al. (2021) propose a deep learning method for the inversion of product radargrams for the study of tunnel linings. The grating specifically targets diffraction hyperbolas to identify the geometry of diffracting elements. The system is trained on synthetic radargrams produced for diffracting elements of various geometries. This method is promising to reconstruct the geometry of these diffracting elements for data produced by the FlyRadar system. However, it will be necessary to produce learning data, on real or synthetic cases.

This project has received funding from the European Union's Horizon 2020 research and innovation programme under MSCA-RISE2020 grant agreement No 101007973.

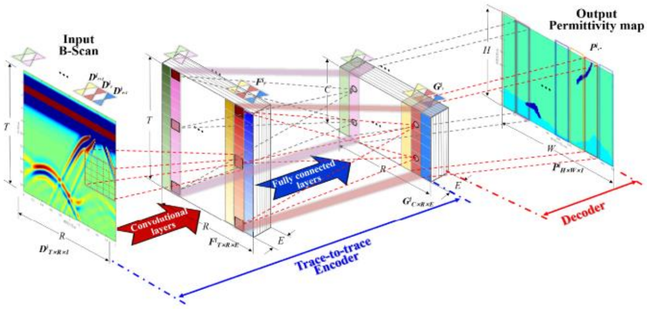

Figure 11: Architecture of the GPRInvNet network. The input data (radargram) is reduced in an encoder and then expanded in a decoder to produce a permittivity section. (Liu et al., 2021).

5. Conclusion

The radargrams produced by the FlyRadar system will need to be inverted to produce the most reliable geometry and permittivity estimates possible. Inversion techniques are based on radar equations that describe how signal strength changes along its path from the transmitter to the target and back to the receiver.

If external data is available, such as the layer thickness measurement for example, it will be possible to estimate the permittivity of these layers from the return times of the signal to the sensor. Other techniques make it possible to jointly invert the geometry and the permittivity from a radargram. These techniques are based either on the characteristics of the diffraction hyperbolas, or on the intensities of the signals picked up by the radar. Other techniques such as deep learning have not yet been used to process geological data. However, they seem promising on the available examples.

This project has received funding from the European Union's Horizon 2020 research and innovation programme under MSCA-RISE2020 grant agreement No 101007973.

6. Bibliography

Alberti, G., Castaldo, L., Orosei, R., Frigeri, A., Cirillo, G.: Permittivity estimation over Mars by using SHARAD data: the Cerberus Palus area, J. Geophys. Res., 117, E09008, doi:10.1029/2012JE004047, 2012.

Berthelier, J. J., et al.: GPR, a ground-penetrating radar for the Netlander mission, J. Geophys. Res., 108(E4), 8027, doi:10.1029/2002JE001866, 2003.

Bramson, A. M., Byrne, S., Putzig, N.E., Sutton, S., Plaut, J.J., Brothers, T.C., Holt, J.W.: Widespread excess ice in Arcadia Planitia, Mars, Geophys. Res.Lett., 42, 6566–6574, doi: 10.1002/2015GL064844, 2015

Brouet, Y., et al.: A laboratory-based dielectric model for the radar sounding of the martian subsurface, Icarus, 321, 960–973, doi: 961 10.1016/j.icarus.2018.12.029, 2019.

ElShafie, A., Heggy, E.: Dielectric and hardness measurements of planetary analog rocks in support of in-situ subsurface sampling, Planetary and Space Science 86, 150–154, doi: 10.1016/j.pss.2013.02.003, 2013.

Ford, J.P., and 8 others: Spaceborne Radar Observations, A Guide for Magellan Radar-Image Analysis: JPL Publication 89-41,126 p., 1989.

Girardi, J.D., Davis, D.M.:Parabolic dune reactivation and migration at Napeague, NY, USA: Insights from aerial and GPR imagery. Geomorphology 114, doi:10.1016/j.geomorph.2009.08.011, 2010.

Grima, C.: Etude de la surface et de la subsurface de Mars par sondage radar. Analyse des données MRO/Sharad. Theses, Université de Grenoble. Français. NNT: 2011GRENU004. tel-00583703, 2011.

Grima, C., Kofman, W., Mouginot, J., Phillips, R.J., Herique, A., Biccari, D., Seu, R., Cutigni, M.: 'North polar deposits of Mars: Extreme purity of the water ice'. Geophysical Research Letters, 36, doi: 10.1029/2008GL036326, 2009.

Heggy, E., et al.: 'Local geoelectrical models of the Martian subsurface for shallow groundwater detection using sounding radars'. Journal of GeophysicalResearch-Planets, 108 (E4), 2003.

Kozlov, A.I., Ligthart, L.P. and Logvin, A.I.: Mathematical and physical modelling of microwave scattering and polarimetric remote sensing: Kluwer academic publishers, 2001.

Liu, B., Ren, Y.,Liu, H., Hui Xu, H., Wang, Z., Cohn, A.G., Jiang, P.: GPRInvNet: Deep Learning-Based Ground-Penetrating Radar Data Inversion for Tunnel Linings, IEEE Transactions on Geoscience and Remote Sensing 99, 1-21, doi: 10.1109/TGRS.2020.3046454, 2021.

Liu, Y., Irving, J., Holliger, K.: High-resolution velocity estimation from surface-based common-offset GPR reflection data. Geophys. J. Int., 230, 131–144, https://doi.org/10.1093/gji/ggac058, 2022.

Looyenga, H.: Dielectric constants of heterogeneous mixtures, Physica, 31(3), 401–406, 1965.

This project has received funding from the European Union's Horizon 2020 research and innovation programme under MSCA-RISE2020 grant agreement No 101007973.

Lynn, P.A.: Radar Systems. Springer, doi: 1-146.10.1007/978-1-4613-1579-7_1, 1986.

Pettinelli, E., Paolo Burghignoli, P., Pisani, A.R., Ticconi, F., Galli, A., Vannaroni, G., Bella F.: Electromagnetic Propagation of GPR Signals in Martian Subsurface Scenarios Including Material Losses and Scattering, IEEE Transactions on Geoscience and Remote Sensing, 45, 5, doi: 10.1109/TGRS.2007.893563, 2007.

Picardi, G., et al.: Marsis data inversion approach: preliminary results, in IEEE National Radar Conference, doi 10.1109/RADAR.2008.4721073, 2008.

Wilhelms, F.: Explaining the dielectric properties of firn as a density-and conductivity mixed permittivity (DECOMP). Geophysical Research Letters, 32 (16), doi 10.1029/2005GL022808, 2005.

This project has received funding from the European Union's Horizon 2020 research and innovation programme under MSCA-RISE2020 grant agreement No 101007973.